Spectrochimica Acta Part A: Molecular and Biomolecular Spectroscopy 97 (2012) 397–405

Contents lists available at SciVerse ScienceDirect

Spectrochimica Acta Part A: Molecular and Biomolecular Spectroscopy

journal homepage: www.elsevier.com/locate/saa

Ligational behavior of Schiff bases towards transition metal ion and metalation effect on their antibacterial activity

Jai Devi, Nisha Batra, Rajesh Malhotra *

Department of Chemistry, Guru Jambheshwar University of Science and Technology, Hisar 125001, Haryana, India

HIGHLIGHTS

- Synthesis of azomethine Schiff base ligands and their metal complexes.
- Ligands and metal complexes were characterized by (IR, UV–VIS, NMR, ESR, Mass) and TGA.
- *In vitro* antibacterial activity at different concentrations of compounds were studied.
- Biocidal activity of the metal complexes increased upon coordination with metal ions.

GRAPHICAL ABSTRACT

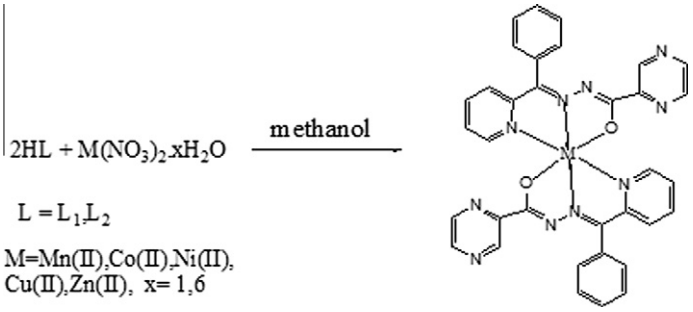

ARTICLE INFO

Article history:
Received 13 March 2012
Received in revised form 5 June 2012
Accepted 19 June 2012
Available online 28 June 2012

Keywords:
Transition complexes
Azomethine
Antibacterial
Inhibition

ABSTRACT

New Schiff bases pyrazine-2-carboxylicacid (phenyl-pyridin-2-yl-methylene)-hydrazide (Hpch-bp) **HL_1** and pyrazine-2-carboxylicacid (pyridin-2-ylmethylene)-hydrazide (Hpch-pc) **HL_2** derived from condensation of pyrazine carboxylic hydrazide (Hpch) with 2-benzoyl pyridine (bp) or pyridine 2-carbaldehyde (pc) and their transition metal complexes of type $ML_{(1-2)2}$ have been synthesized, where M = Mn(II), Co(II), Ni(II), Cu(II) and Zn(II). Characterization of ligands and their metal complexes was carried out by elemental analysis, conductimetric studies, magnetic susceptibility, spectroscopic techniques (IR, UV–VIS, NMR, ESR, Mass) and thermogravimetric analysis. The physico-chemical studies revealed octahedral geometry or distorted octahedral geometry around metal ion. These azomethine Schiff base ligands acted as tridentate O N N coordinating through carbonyl, azomethine and pyridine nitrogen present in the ligand. The thermodynamic and thermal properties of the complexes have been investigated and it was observed on the basis of these studies that thermal stability of complexes follows the order Mn < Zn < Cu < Co < Ni. The ligands and their complexes were tested for *in vitro* antibacterial activity at different concentrations against bacteria viz. Gram positive *Bacillus subtilis*, *Micrococcus luteus* and Gram negative *Pseudomonas aeruginosa*, *Pseudomonas mendocina*. A marked enhancement in biocidal activity of the ligands under similar experimental conditions was observed as a consequence of coordination with metal ions. The trend of growth inhibition in the complexes was found to be in the order: Cu > Mn > Ni > Co > Zn.

Introduction

The Schiff base have been most widely used versatile ligands, in their neutral or deprotonated forms to form stable complexes with most of the transition metal ions and still play an important role in metal coordination chemistry even after almost a century since their discovery. This class of compounds has been explored as models for biological systems [1] and has attracted attention of biological chemists due to their wide ranging pharmacological properties including antimicrobial [2–4], anti-tuberculosis and anti-tumor activity [5–7], herbicidal, insecticidal and as plant growth regulators. It has been reported that many compounds possess modified pharmacological and toxicological potentials when

* Corresponding author. Tel.: +91 9896608818; fax +91 1662276240.
E-mail address: malhotra_ksrk@yahoo.co.in (R. Malhotra).

1386-1425/$ - see front matter © 2012 Elsevier B.V. All rights reserved.
http://dx.doi.org/10.1016/j.saa.2012.06.026

combined with metal ions [8]. The remarkable enhancement in the biological activity of acid hydrazides and their corresponding aroyl hydrazones is due to their ability to bind with transition metal ions in living systems. Tridentate and tetradentate Schiff base ligands are of particular interest not only for existing in lactam (keto) or lactim (enol) tautomeric forms giving variations to donating properties of these ligands to form complexes with unusual coordination numbers [9], high thermodynamic stability and kinetic inertness but also for their ability to exhibit catalytic and magnetic properties and to mimic biological sites upon complexation with metal ions. The activity of metal complexes in biological systems depends on the ease of cleavage of bond between metal ion and the ligand for which it is important to understand their coordination behavior and relationship between metal and the ligands in various biological systems. Considering the importance and properties of the Schiff base hydrazones and their metal complexes, present work describes synthetic, spectroscopic, thermal aspects and particularly antibacterial activity of transition metal complexes of the Schiff base obtained from condensation of pyrazine carboxylic hydrazide with 2-benzoyl pyridine or pyridine 2-carbaldehyde.

Experimental

Materials and methods

All the chemicals used were obtained through Aldrich and used as such without any further purification. IR spectra were recorded on Shimadzu IR affinity-I 8000 FT-IR spectrometer using KBr disc having wavelength range of 4000–400 cm^{-1}. ^1H NMR and ^{13}C NMR spectra were recorded on Bruker Avance II 300 MHz NMR spectrometer and the chemical shifts were reported in parts per million relative to TMS as internal standard in $CDCl_3$. UV spectra were recorded on UV–VIS–NIR Varian Cary-5000 spectrometer in DMF. Magnetic susceptibilites of complexes were measured by Gouy's method, using Hg $[Co(SCN)_4]$ as the calibrant at room temperature. ESR spectra of the copper complexes were recorded on a Varian E112 X-band spectrometer using tetracyanoethylene (TCNE) as the internal standard. Molar conductance measurements of a 10^{-3} M solution of metal complexes in DMF at room temperature were carried out using a model-306 Systronics conductivity bridge. Elemental analysis was carried out on Perkin Elmer 2400. Thermogravimetric (TG) analysis of samples at a heating rate of 10 °C min^{-1} was carried out using Perkin Elmer Diamond TG/DTA thermogravimetric analyzer instrument under high purity argon atmosphere at a flow rate of 20 ml min^{-1}. Mass spectra were recorded on API 2000 (Applied Biosystems) mass spectrometer equipped with an electrospray source and a Shimadzu Prominence LC.

Synthesis of the Schiff bases

Pyrazine-2-carboxylic acid (phenyl-pyridin-2-yl-methylene)-hydrazide (Hpch-bp) **HL_1**. To the solution of pyrazine carboxylic acid hydrazide (0.55 g, 4 mmol) in methanol (30 mL) was added dropwise with continuous stirring, a solution of 2-benzoyl pyridine (0.73 g, 4 mmol) in the same solvent. The reaction mixture was then refluxed for 5 h. The solid product so obtained was filtered and recrystallised in hot methanol. The same method was adopted to prepare other ligand (Hpch-pc) **HL_2**.

Synthesis of the metal complexes

Metal complexes were prepared by dropwise addition of 10 mL methanolic solution of the metal salt to 20 mL methanolic solution of Schiff base (2 mmol) with continuous stirring. The resulting

Table 1
Analytical data of compounds.

Sr. no.	Compounds	Mol. formula (mol.wt. an)	Yield (%)	M.Pt.[a]	Color	Found (calcd) (%)					*m/z* molecular ion peak	(Ω_M) Molar conductance $\times 10^{-3}$	Magnetic moment μ_{eff} (BM)
						C	H	N	O	M			
1	HL_1	$C_{17}H_{13}N_5O$ (303.32)	75	165	White	67.32 (67.51)	4.52 (4.44)	23.09 (23.21)	5.27 (5.39)	–	303.8	–	–
2	HL_2	$C_{11}H_9N_3O$ (227.08)	72	125	White	58.44 (58.27)	3.99 (4.11)	31.72 (30.95)	7.04 (7.16)	–	227.2	–	–
3	$Mn(L_1)_2$	$C_{34}H_{24}N_{10}O_2Mn$ (659.56)	62	–	Orange	61.21 (61.01)	3.67 (3.69)	21.24 (21.37)	4.85 (4.98)	8.33 −8.67	659.7	2.2	5.9
4	$Co(L_1)_2$	$C_{34}H_{24}N_{10}O_2Co$ (663.14)	58	–	Green	61.94 (61.83)	3.65 (3.78)	21.81 (21.55)	4.82 (5.01)	8.88 −9.01	663.4	2.7	4.53
5	$Ni(L_1)_2$	$C_{34}H_{24}N_{10}O_2Ni$ (662.14)	60	–	Brown red	61.76 (61.62)	3.65 (3.98)	21.42 (21.26)	4.82 (4.95)	8.85 −8.98	662.3	1.9	2.8
6	$Cu(L_1)_2$	$C_{34}H_{24}N_{10}O_2Cu$ (668.17)	65	–	Dark green	61.12 (61.31)	3.92 (3.85)	20.46 (20.38)	5.05 (4.98)	9.51 −9.74	668.3	2.6	1.9
7	$Zn(L_1)_2$	$C_{34}H_{24}N_{10}O_2Zn$ (668.13)	62	–	Color-less	60.95 (60.74)	3.61 (3.94)	20.91 (21.04)	4.78 (4.91)	9.76 −9.69	668.4	1.5	–
8	$Mn(L_2)_2$	$C_{22}H_{16}N_{10}O_2Mn$ (507.08)	61	–	Orange	52.68 (52.41)	3.18 (3.31)	27.61 (27.85)	6.81 (6.74)	10.83 −10.97	507.1	2.4	5.8
9	$Co(L_2)_2$	$C_{22}H_{16}N_{10}O_2Co$ (511.07)	62	–	Green	51.67 (51.83)	3.35 (3.28)	27.69 (27.62)	6.36 (6.68)	11.82 −11.75	511.2	2.6	4.48
10	$Ni(L_2)_2$	$C_{22}H_{16}N_{10}O_2Ni$ (510.08)	63	–	Brown red	51.7 (51.98)	3.16 (3.2)	27.9 (27.83)	6.76 (6.59)	11.48 −11.83	510.2	1.8	2.78
11	$Cu(L_2)_2$	$C_{22}H_{16}N_{10}O_2Cu$ (515.08)	59	–	Dark green	51.21 (51.53)	3.13 (3.37)	27.15 (27.09)	6.2 (6.42)	12.42 −12.55	515.2	2.7	1.9
12	$Zn(L_2)_2$	$C_{22}H_{16}N_{10}O_2Zn$ (516.07)	59	–	Color-less	51.03 (51.24)	3.41 (3.24)	27.15 (27.29)	6.38 (6.29)	12.93 −12.86	516.3	1.9	–

[a] Complexes $M(L_{1-2})_2$ have no sharp melting point, but decomposes >250 °C.

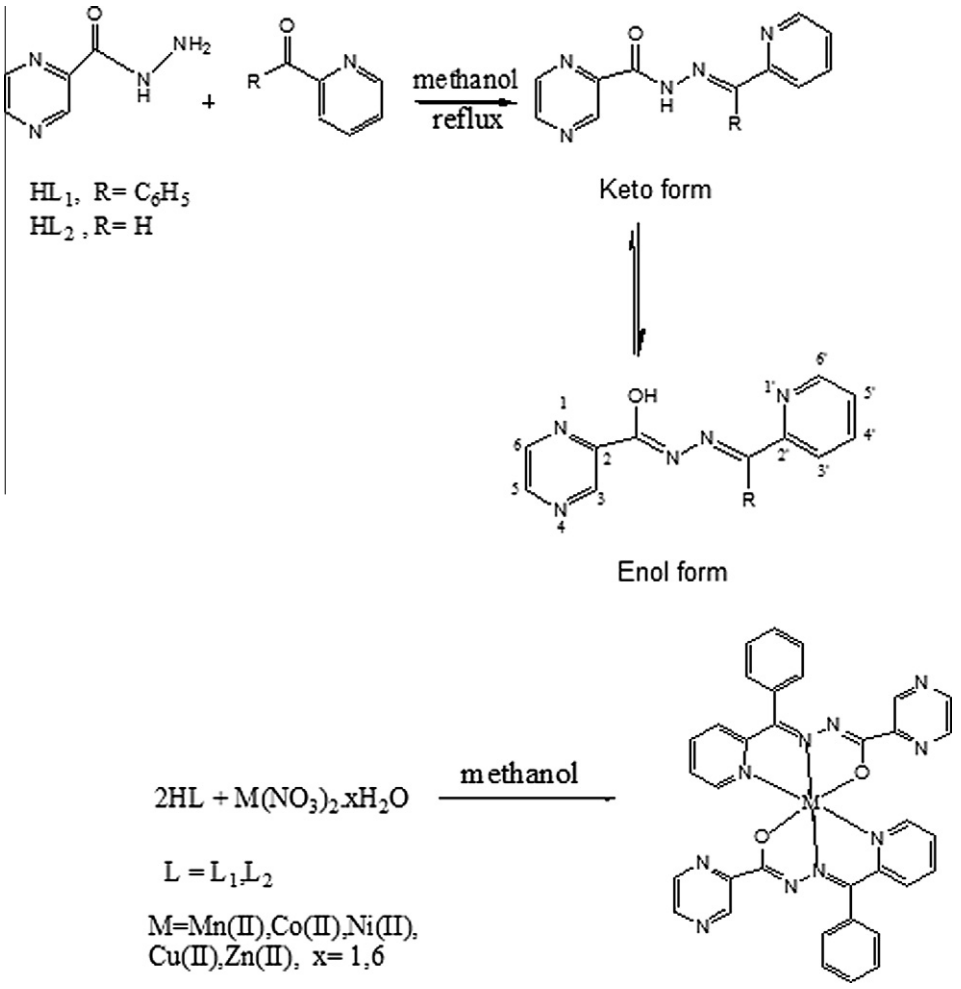

Fig. 1. Scheme for synthesis of ligand and their metal complexes.

Table 2
Infrared spectra of compounds.

Sr. no.	Ligand/complexes	υ(N–H)	υ(C–O)	υ(C-O)	υ(C=N)	υ(M–O)	υ(M–N)	υ(Py)
1	HL_1	3350	1681	–	1580	–	–	693
2	HL_2	3361	1695	–	1577	–	–	693
3	$Mn(L_1)_2$	–	–	1074	1547	434	501	700
4	$Co(L_1)_2$	–	–	1086	1556	441	499	695
5	$Ni(L_1)_2$	–	–	1065	1545	435	503	694
6	$Cu(L_1)_2$	–	–	1090	1538	427	509	702
7	$Zn(L_1)_2$	–	–	1083	1549	438	501	699
8	$Mn(L_2)_2$	–	–	1078	1544	431	509	699
9	$Co(L_2)_2$	–	–	1072	1553	439	511	694
10	$Ni(L_2)_2$	–	–	1071	1542	428	505	696
11	$Cu(L_2)_2$	–	–	1086	1536	429	499	701
12	$Zn(L_2)_2$	–	–	1074	1546	442	509	698

Table 3
^1H and ^{13}CNMR of ligands and their zinc complexes.

Ligands	^1H NMR ($CDCl_3$) δ in ppm	^{13}C NMR ($CDCl_3$) δ in ppm
HL_1	15.08(s, NH proton), 9.50(s, 1H, C_3–H), 8.93 (J = 3.3, d, C_6–H), 8.77(J = 2.1, d, C_6–H), 8.62(J = 2.1, d, C_5–H), 7.84 (J = 7.8, d, 1H, C_3–H), 7.67 (J = 9.0, J = 3.3, dd, C_4-H, C_5-H), 7.48–7.28 (m, 5H, Ph-H)	162.47 (C=O), 152.53 (C=N), 149.20 (C_2), 148.85(C_6), 148.18(C_2), 147.90(C_5), 137.84(C_3), 137.46(C_6), 136.94(C_4), 135.97($C_{5'}$), 129.63–128.45(Ph-C), 127.10($C_{3'}$)
HL_2	15.77(s, NH proton), 12.20(s, –CH proton), 9.20(s, C_3-H), 8.82 (J = 2.8, d, C_6–H), 8.76 (J = 3.3, d, C_6-H), 8.61(J = 3.3, d, C_5-H), 7.80 (J = 2.7, d, C_3-H), 7.56 (J = 9.4, J = 2.1, dd, C_4-H, C_5-H)	162.33(C=O), 152.33(C=N), 148.80(C_2), 148.54(C_6), 148.03(C_2), 147.71(C_5), 137.96(C_3), 136.13(C_6), 135.48(C_4), 135.04($C_{5'}$), 126.05($C_{3'}$)
$Zn(L_1)_2$	9.15(s, C_3-H), 8.81 (J = 4.8, d, C_6-H), 8.30(J = 6.0, d, C_6–H), 8.04 (J = 6.0, d, C_5-H), 7.50 (J = 3.3, d, C_3-H), 7.43 (J = 7.8, J = 2.1, dd, C_4-H, C_5–H), 7.65–7.56 (m, 5H, Ph-H)	163.34(C=O), 154.32(C=N), 149.28(C_2), 149.05(C_6), 147.78(C_2), 147.50(C_5), 138.44(C_3), 137.84(C_6), 137.04(C_4), 136.07($C_{5'}$), 130.08–128.45(Ph-C), 128.10($C_{3'}$)
$Zn(L_2)_2$	12.29(s,-CH proton), 9.08(s, 1H, C_3-H), 8.85 (J = 3.8, d, C_6-H), 8.50(J = 4.2, d, C_6–H), 8.44 (J = 4.2, d, C_5-H), 7.75 (J = 4.4, d, C_3-H), 7.52 (J = 9.0, J = 2.1, dd, C_4-H, C_5–H)	162.44(C=O), 153.45(C=N), 148.28($C_2$148.15(C_6), 147.97(C_2), 147.50(C_5), 138.92(C_3), 136.84(C_6), 135.04(C_4), 135.01($C_{5'}$), 127.10($C_{3'}$)

solution was refluxed for 2 h. The precipitate separated out during refluxing was filtered and washed with hot methanol, finally with petroleum ether and then dried.

Methodology of antibacterial activity

In vitro antibacterial activity of ligands and their complexes were assessed against a series of Gram positive *Bacillus subtilis*, *Micrococcus luteus* and Gram negative *Pseudomonas aeruginosa*, *Pseudomonas mendocina* using agar plate disc method [10–11]. Stock solution was made by dissolving compound in 10 mL of DMSO. The media was made by dissolving Nutrient agar (15 g) in 1 L distilled water. The mixture was autoclaved for 15 min at 120 °C and then dispensed into sterilized Petri dishes, allowed to solidify and then used for inoculation. Target microorganisms cultures were prepared separately in 15 ml of liquid Nutrient agar for activation. Inoculation was done with the help of micropipette with sterilized tips, 100 μl of activated strain was placed onto the surface of agar plate, spread over the whole surface and then two wells having diameter of 10 mm were dug in media. Sterilized stock solutions were used for the application in the well of inoculated agar plates. In this well of inoculated agar plates 100 μl of solution was poured and incubated at 37 °C for 48 h. Activity was determined by measuring the diameter of zone showing complete inhibition and has been expressed in mm. All this experiments were performed in triplicate.

Table 4
Electronic spectra of compounds.

Sr. no.	Ligands/ complexes	Absorption (cm^{-1})	Band assignment	Geometry
1	HL_1	31,250	INCT[b]	–
2	HL_2	30,959	INCT[b]	–
3	$Mn(L_1)_2$	25,839	$n\rightarrow\pi^*$	Octahedral
4	$Co(L_1)_2$	23,415	$^4T_{1g}(F)\rightarrow{}^4T_{1g}(P)$	Octahedral
		15,391	$^4T_{1g}(F)\rightarrow{}^4A_{2g}(F)$	
		9826	$^4T_{1g}(F)\rightarrow{}^4T_{2g}(F)$	
5	$Ni(L_1)_2$	24,839	$^3A_{2g}(F)\rightarrow{}^3T_{1g}(P)$	Octahedral
		15,977	$^3A_{1g}(F)\rightarrow{}^3T_{1g}(F)$	
		10,873	$^3A_{2g}(F)\rightarrow{}^3T_{2g}(F)$	
6	$Cu(L_1)_2$	25,510	π N$\rightarrow$Cu*	Distorted
		16,492	$^2E_g(D)\rightarrow{}^2T_{2g}(D)$	Octahedral
7	$Zn(L_1)_2$	23,445	LMCT	Octahedral
8	$Mn(L_2)_2$	25,745	$n\rightarrow\pi^*$	Octahedral
9	$Co(L_2)_2$	23,126	$^4T_{1g}(F)\rightarrow{}^4T_{1g}(P)$	Octahedral
		15,267	$^4T_{1g}(F)\rightarrow{}^4A_{2g}(F)$	
		9785	$^4T_{1g}(F)\rightarrow{}^4T_{2g}(F)$	
10	$Ni(L_2)_2$	24,779	$^3A_{2g}(F)\rightarrow{}^3T_{1g}(P)$	Octahedral
		15,945	$^3A_{1g}(F)\rightarrow{}^3T_{1g}(F)$	
		10,783	$^3A_{2g}(F)\rightarrow{}^3T_{2g}(F)$	
11	$Cu(L_2)_2$	25,467	π N$\rightarrow$Cu*	Distorted
		16,473	$^2E_g(D)\rightarrow{}^2T_{2g}(D)$	Octahedral
12	$Zn(L_2)_2$	24,547	LMCT	Octahedral

[b] INCT – intranuclear charge transfer; LMCT – ligand to metal charge transition.

Results and discussion

The ligands have been synthesized by condensation of pyrazine carboxylic hydrazide with 2-benzoyl pyridine or pyridine 2-carbaldehyde. The homogeneity of these compounds was regularly checked by TLC. The reaction of these ligands with metal salts in 1:2 molar ratio in dry methanol afford metal complexes of type $ML_{(1-2)2}$. All these metal complexes have been obtained as colored solid, stable on prolonged exposure to air and insoluble in most of common organic solvents expect in DMF and DMSO. The analytical data of the ligands and complexes together with other physical properties are summarized in Table 1. The molar conductivity of metal complexes in DMSO has low value 1.8–2.7 $ohm^{-1}\ cm^2\ mol^{-1}$ indicating non electrolytic nature. The geometry of these metal complexes has been determined using spectroscopic techniques (IR, Electronic, ESR and Mass). The ligand was chelated to all the metal ions in enolic form with the replacement of one hydrogen atom as shown in Scheme (Fig. 1).

Infrared spectra

IR spectra of complexes were analysed in comparison to free ligands (HL_1&HL_2) and the coordination sites were ascertained on the basis of shifts in the frequencies of various groups and/or from the intensity lowering. In the IR spectrum of the ligands strong band at 1681–1695 cm^{-1} and 3350–3361 cm^{-1} were due to υ(C=O) and υ(N–H) bands, respectively. The absence of these bands in the spectra of complexes indicated that hydrazone ligand has coordinated to metal center through carbonyl oxygen after deprotonation. This evidence was strengthened by presence of new stretching vibrations between 1097 and 1050 cm^{-1} attributed

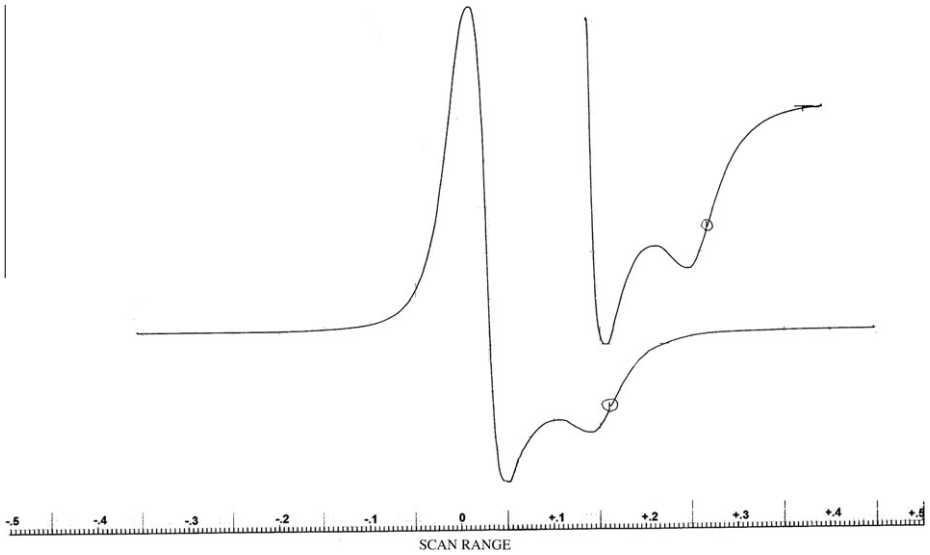

Fig. 2. ESR spectra of Cu(II) complex at 300 K.

to υ(C–O) in the complexes. The IR spectra of complexes displayed absorption bands at 1536–1556 cm^{-1} which can be assigned to C=N streching frequencies of coordinated ligands, whereas for free ligands these bands were at 1577–1580 cm^{-1}. The shift to lower frequencies (as compared to free ligand) indicated donation of the lone pair of electrons on azomethine nitrogen to metal center, this has been strengthened by the shift of υ(N–N) band from 1050 to 1070 cm^{-1} in free ligands to 1025–1070 cm^{-1} in complexes and supported by the presence of M–O and M–N bands at 427–440 cm^{-1} and 480–510 cm^{-1}, respectively [12] in the complexes. Low energy pyridine ring in plane and out of plane vibrations observed in spectrum of ligands at 693–698 cm^{-1} were shifted to higher frequencies at 694–702 cm^{-1} on complexation indicated that heterocyclic nitrogen (1) of pyridine ring was involved in coordination [13] (Table 2).

^{1}H and ^{13}C NMR spectra

The NMR (^{1}H and ^{13}C) spectra of ligands/zinc(II) complexes were recorded in $CDCl_3$/$CDCl_3$ containing small amount of DMSO-d_6, with tetramethylsilane as internal reference and data is given in Table 3. ^{1}H NMR of ligands showed singlet at 15.08 ppm due to azomethine proton and one singlet at 9.50 ppm due to proton attached to C_3. The aromatic protons appeared as doublet and multiplet in the range at 8.93–7.28 ppm. A comparative study of ligands and Zn(II) complexes revealed the ligational behavior of the ligand. The absence of peak at 15.08 ppm indicated deprotonation of –NH proton (via enolization) and the shift in protons of pyridine ring were also observed. In ^{13}C NMR of ligand carbonyl carbon showed signal at 162.57 ppm, azomethine carbon at 152.53 ppm and aromatic carbons in between 149.20 and 127.10 ppm. The signals due to carbonyl and azomethine carbons were slightly shifted downfield in comparison to the corresponding signals of these groups in the ligands thereby confirming the complexation with zinc metal ion. It was observed that DMSO did not have any coordinating effect on the spectra of zinc complexes.

Table 5
ESR data of copper(II) complexes.

Complex	$g_{\|}$	$g_{\perp}$	g_{av}	G	λ	α^2	β^2
$Cu(L_1)_2$	2.31	2.07	2.15	4.54	618	0.65	0.97
$Cu(L_2)_2$	2.29	2.06	2.13	4.24	535	0.63	0.96

Electronic spectra

Electronic spectra of complexes were recorded in DMF and compared with that of corresponding ligands. In the electronic spectra of Mn(II) complexes band due to $n\rightarrow\pi^*$ transition was appeared in the range of 25,745–25,839 cm^{-1} confirming their octahedral geometry whereas d–d transition was not observed probably for low intensities for these complexes. In the electronic spectra of Co(II) complexes and Ni(II) complexes three bands in the vicinity of 10,000 cm^{-1}, 17,000 cm^{-1}, 24,000 cm^{-1} (Table 4) have been assigned due to $^{4}T_{1g}(F)\rightarrow{}^{4}T_{2g}(F)$, $^{4}T_{1g}(F)\rightarrow{}^{4}A_{2g}(F)$, $^{4}T_{1g}(F)\rightarrow{}^{4}T_{1g}(P)$ and $^{3}A_{2g}(F)\rightarrow{}^{3}T_{2g}(F)$, $^{3}A_{1g}(F)\rightarrow{}^{3}T_{1g}(F)$, $^{3}A_{2g}(F)\rightarrow{}^{3}T_{1g}(P)$ respectively, which was in accordance with octahedral geometry around cobalt and nickel ion [14]. In the electronic spectra of Cu(II) complexes bands in vicinity of 25,000 cm^{-1} and 16,000 cm^{-1} were due to charge transfer and $^{2}E_g\rightarrow{}^{2}T_{2g}$ transition, respectively. In the electronic spectra of Cu(II) complexes broadness of band occur due to Jahn-Teller distortion, indicating the distortion from octahedral geometry [15]. In the electronic spectrum of Zn(II) complexes only one band was observed due to LMCT transition.

ESR spectra of copper complexes

ESR spectra of copper complexes were recorded in DMSO at 300 K (Fig. 2). The observed value for Cu(II) complex with ligand HL_1 was $g_{\perp}$ = 2.07 and $g_{\|}$ = 2.29 while for Cu(II) complex with ligand HL_2 it was $g_{\perp}$ = 2.06 and $g_{\|}$ = 2.26 (Table 5). The anisotropic G value have been calculated by using $G = (g_{\|} - 2.0023)/(g_{\perp} - 2.0023)$ giving idea for exchange interactions between Cu(II) centers. Since in these complexes G = 4.24 and 4.46 indicated that there was no exchange in the copper complexes and hence distorted octahedral geometry proposed for Cu(II) complexes [16]. Moreover, the value of $g_{\|} > g_{\perp} > 2.0023$ which is in accordance with

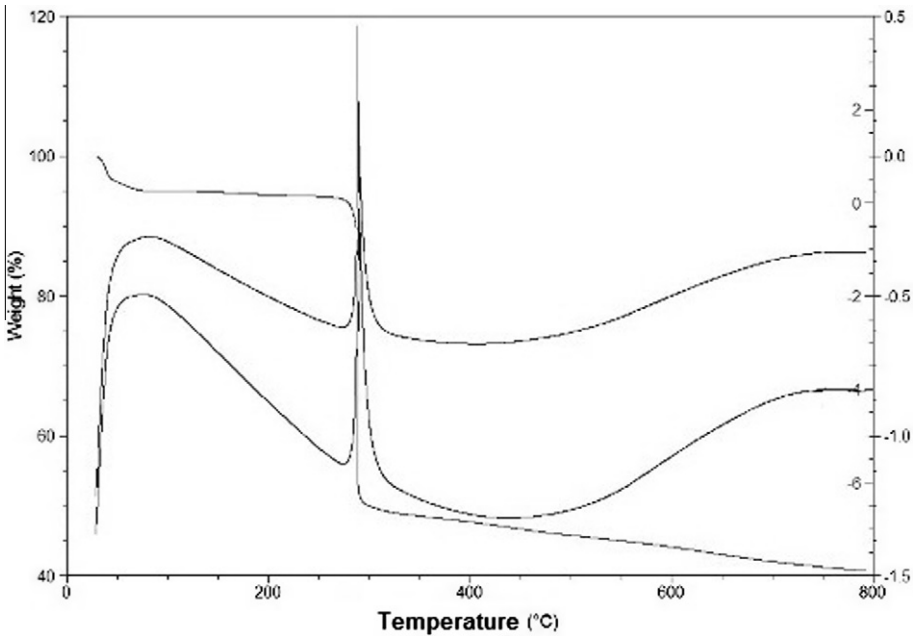

Fig. 3. TG/DTG curve of complex $Zn(L_1)_2$.

axially elongated octahedral geometry and indicated that unpaired electron present in $d_{x^2-y^2}$ ground state of Cu(II) [17]. The spin orbital coupling constant λ was calculated using the relation $g_{av} = 2(1-2\lambda/10Dq)$, $g_{av}=1/3(g_{||} + 2g_{\perp})$ which is less than Cu(II) λ (832 cm^{-1}) free ion complex supported the covalent character of M–L bond in complex. The molecular orbital coefficients, in-plane π bonding (β^2) and in-plane σ bonding (α^2) have been calculated using relations [18] (Table 5). The observed value of covalency parameter α^2 (0.65) indicated that the complex has some covalent character in ligand environment, if the value of $\alpha^2 = 0.5$, it indicates complete covalent bonding, while the value of $\alpha^2 = 1.0$ suggest complete ionic bonding. From these value of $\alpha^2 = 0.65$ and $\beta^2 = 0.97$, it was evident that there is an interaction in in-plane σ bonding (α^2), where as in-plane π bonding (β^2) is almost ionic [19].

Magnetic susceptibility measurements

The observed magnetic moment for the transition metal complexes are generally diagnostic of the coordination geometry around metal ion. The effective magnetic moment was calculated using the relation $\mu_{eff} = 2.828(X_mT)^{1/2}$ BM, where X_m is molar susceptibility. Mn (II) complexes showed magnetic moment values in the range 5.8–5.9 BM which was expected for high spin d^5 system having octahedral geometry. The effective magnetic moment values of 4.4–4.5 BM for Co(II) complexes corresponded to the presence of three unpaired electrons indicating a quartet ground state, which was orbitally triply degenerated and would cause an angular moment contribution to magnetic moment, Ni(II) complexes showed magnetic moment 2.8 BM corresponding to two unpaired electrons indicating a triplet ground state having octahedral geometry around metal ion. Cu(II) complexes showed magnetic moment 1.9 BM which was due to one unpaired electron and suggested octahedral geometry of the complexes and Zn(II) complexes were found to be diamagnetic as expected for d^{10} configuration.

Mass spectra

Mass spectra of Schiff base ligands and their complexes showed molecular ion peaks which were in agreement with their molecular formula (Table 1). The molecular ion peak for the ligand HL_1 ($C_{17}H_{13}N_5O$) and its corresponding cobalt complex ($CoC_{34}H_{24}N_{10}O_2$) observed at *m/z* 303.8 and 663.4, respectively. The purity of the ligands and their complexes were checked using LC-mass technique.

Thermogravimetric analysis

Thermal behaviors of complexes were investigated by TG/DSC techniques. The thermogravimetric analysis for the complexes was carried out within temperature ranging from room temperature to 800 °C. The TG/DTG curve of complex $ZnL_{(1)2}$ is given in Fig. 3.

Table 6
Kinetic parameters of complexes.

Sr. no.	Compounds	Decomposition range (°C)	E (KJ mol^{-1})	ΔH (KJ mol^{-1})	ΔS (J mol^{-1} K^{-1})	ΔG (KJ mol^{-1})
1	$Mn(L_1)_2$	50–280	34.62	69.72	−9.87	72.06
		280–500	87.31	78.94	−15.73	85.51
		500–780	92.12	94.32	−18.36	105.96
2	$Co(L_1)_2$	50–280	68.1	103.02	−13.04	68.1
		280–500	92.08	81.04	−45.81	92.08
		500–780	116.04	124.08	−32.14	116.04
3	$Ni(L_1)_2$	50–280	62.4	81.13	−25.4	62.4
		280–500	104.21	105.04	−43.51	104.21
		500–780	128.04	91.05	−58.12	128.04
4	$Cu(L_1)_2$	50–280	59.4	61.84	−17.4	85.91
		280–500	95.21	107.6	−13.53	111.86
		500–780	112.1	95.16	−15.58	104.58
5	$Zn(L_1)_2$	50–280	45.76	105.6	−11.28	108.05
		280–500	90.44	83.58	−21.35	91.71
		500–780	103.21	103.4	−18.34	114.31
6	$Zn(L_2)_2$	50–280	40.32	136.3	−12.04	138.88
		280–500	78.12	103.4	−14.05	108.61
		500–780	102.16	105.6	−20.06	115.87

Table 7
In vitro antibacterial activity of ligands and their complexes.

	Compounds	Zone of inhibition (mm)															
		Gram +ve								Gram –ve							
		B. subtilis				*M. Luteus*				*P. aeruginosa*				*P. mendocina*			
		25	50	100	200	25	50	100	200	25	50	100	200	25	50	100	200
1	HL_1	9	12	13	15	11	13	15	18	8	10	11	13	10	11	13	18
2	HL_2	8	10	11	14	8	10	11	14	10	11	12	14	8	9	10	13
3	$Mn(L_1)_2$	17	18	20	21	16	18	21	21	15	17	19	21	17	18	20	23
4	$Co(L_1)_2$	13	15	16	19	13	15	17	18	11	13	14	17	13	15	16	18
5	$Ni(L_1)_2$	14	17	19	21	16	19	20	21	14	16	18	20	16	17	19	22
6	$Cu(L_1)_2$	18	20	22	23	15	17	21	22	16	18	20	23	18	20	22	24
7	$Zn(L_1)_2$	12	13	15	17	12	13	16	18	9	11	13	16	11	13	14	17
8	$Mn(L_2)_2$	14	16	19	20	13	15	18	20	13	15	16	19	11	13	15	18
9	$Co(L_2)_2$	10	12	15	17	10	13	14	16	10	11	12	15	10	12	14	16
10	$Ni(L_2)_2$	15	16	18	19	13	15	17	20	11	13	14	18	12	14	16	19
11	$Cu(L_2)_2$	16	19	21	22	15	16	20	22	15	17	19	22	15	18	20	22
12	$Zn(L_2)_2$	10	13	14	17	10	11	13	16	9	10	11	14	10	11	13	14
13	Streptomycin	19	21	25	26	19	20	23	25	20	23	25	28	22	25	27	30

All the complexes were stable up to 250 °C as no mass loss was observed below 250 °C, eliminated the possibility of water molecule outside the coordination sphere.

In general, the stages of thermal decomposition of the complexes can be written as shown:

$$M(L_{1-2})_2 \xrightarrow{50-250\ ^\circ C} \text{No hydrated water}$$

[M=Mn(II), Co(II), Ni(II), Cu(II) and Zn(II)]

$$M(L_{1-2})_2 \xrightarrow{250-500\ ^\circ C} \text{Intermediate (unstable)}$$

$$\text{Intermediate} \xrightarrow{500-800\ ^\circ C} \text{Metal oxide}$$

Intermediates formed in the subsequent steps ultimately have undergone violent decomposition to give the respective metal oxides. The thermodynamic activation parameters of decomposition processes of dehydrated complexes namely activation energy (E), enthalpy (ΔH), entropy (ΔS) and free energy of decomposition (ΔG) (Table 6), were evaluated by employing the Coats–Redfern method [20] and were helpful in assigning the strength of the complexes. It was found that the thermal stabilities of the complexes of ligand HL_1 follows the order Mn < Zn < Cu < Co < Ni. Complexes of ligand HL_1 with Zn(II) ion were more stable as compared to complex of ligand HL_2 with same metal ions.

Antimicrobial results

Determination of *in vitro* antimicrobial activity of the hydrazones and their corresponding metal complexes are given in Table 7 and their graphical representation in Figs. 4 and 5. Antibacterial studies were done by the agar plate disc method on the following strains i.e., Gram positive *Bacillus subtilis*, *Micrococcus luteus* and Gram negative *Pseudomonas aeruginosa*, *Pseudomonas mendocina* using different concentration of ligands and their complexes (25, 50, 100, 200 μg/mL). Streptomycin was used as a standard drug for antibacterial activity.

It may be concluded from the antimicrobial activity data that:

(i) the antimicrobial activity of ligands and their complexes was due to the presence of toxophorically important imine or carbonyl groups. The mode of action of these compounds may involve the formation of hydrogen bond through

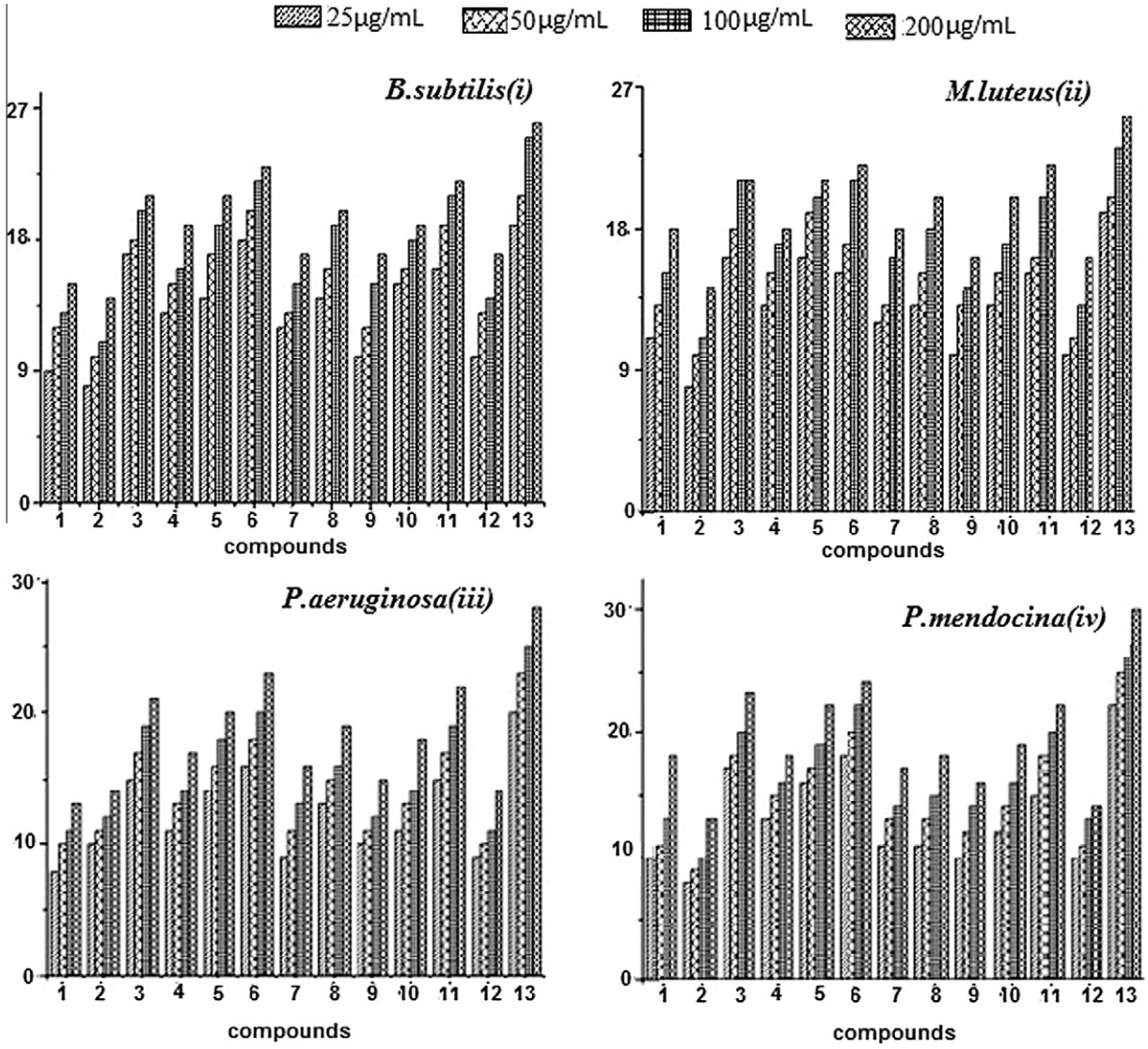

Fig. 4. Antibacterial activity data of ligands and their transition metal complexes (1–12 as in Table 7).

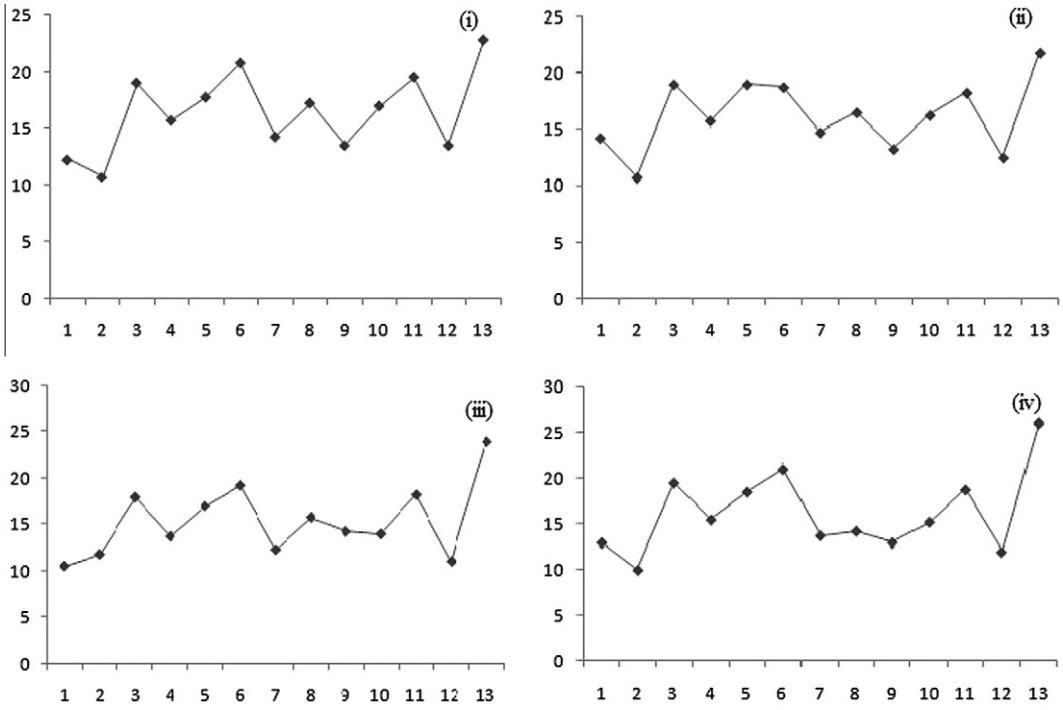

Fig. 5. Average antibacterial activity data of ligands and their transition metal complexes.

azomethine/carbonyl group with the active center of cell constituents, there by resulting in interference with normal cell process.

(ii) A marked enhancement of *in vitro* biocidal studies of the ligands was exhibited on coordination with metal ion against all microorganisms strains under tested identical experimental conditions. The increase in antimicrobial activity may be explained on basis of fact that on chelation the polarity of metal ion is reduced due to overlap of ligand orbital and sharing of positive charge of metal ion with donor groups. Further it increases delocalization of chelate ring and increases the lipophilicity of complexes. This increased lipophilicity enhances penetration of complexes there by disturbing the respiration process of cell and blocking the synthesis of proteins, which further restricts growth of organisms.

(iii) Ligand HL_1 was found to be more potent as compared to HL_2 (except in *Pseudomonas aeruginosa*) which may be due to fact that phenyl ring is electron releasing thereby increasing electron density over azomethine nitrogen and therefore have comparatively stronger interactions with active centers of cell constituents.

(iv) Complexes of HL_1 with divalent transition metal ion were found to be more active as compared to complexes of HL_2. Among these complexes Copper(II) complexes were found to be most active, compared to other complexes. The trend of growth inhibition in the complexes was found to be in the order: Cu > Mn > Ni > Co > Zn.

(v) It is evident from the data that the complexes were more toxic towards Gram (+) strains as compared to Gram (−) strains which may be attributed to the fact that the cell wall of Gram (−) strains have more antigenic properties due to the presence of an outer lipid membrane of lipopolysaccharides.

(vi) Some of compounds have activity close or equal to standard drug. It was clear from the data that compounds with lower concentration were proportionately more potent as compared to same compound with higher concentration.

Conclusion

Tridentate O N N Schiff base ligands have been synthesized and coordinated to divalent metal ions through azomethine nitrogen, carbonyl oxygen and nitrogen of pyridine ring forming stable complexes of ML_2 type with octahedral geometry for Mn(II), Co(II) and Ni(II) ions while with Cu(II) ions distorted octahedral geometry has observed. Ligands and their complexes were evaluated for antimicrobial activity (*in vitro*) of the hydrazones and their corresponding metal complexes. These complexes were found to be more active than respective ligands under identical conditions. Among these complexes Copper(II) complexes were found to be most active, compared to other complexes.

Acknowledgments

Nisha Batra is thankful to Department of Science and Technology, Panchkula Haryana for providing HSCST-JRF fellowship vide letter No. HSCST/4117 on dated 11/11/10.

Appendix A. Supplementary data

Supplementary data associated with this article can be found, in the online version, at http://dx.doi.org/10.1016/j.saa.2012.06.026.

References

[1] S.K. Bharti, S.K. Patel, G. Nath, R. Tilak, S.K. Singh, Trans. Met. Chem. 35 (2010) 917–925.
[2] R. Malhotra, J. Mehta, K. Bala, A.K. Sharma, Ind. J. Chem. 47A (2008) 58–61.
[3] V.B. Badwaik, R.D. Deshmukh, A.S. Aswar, J. Coord. Chem. 62 (12) (2009) 2037–2047.
[4] N. Raman, R. Jeyamurugan, B. Rajkapoor, V. Magesh, Appl. Organometal. Chem. 23 (2009) 283–290.
[5] S. Rollas, S.G. kucukguzel, Molecules 12 (2007) 1910–1939.
[6] G.A. Al. Hazmi, A.A. El. Asmy, J. Coord. Chem. 62 (2009) 337–345.
[7] Y.L. Sang, X.S. Lin, J. Coord. Chem. 63 (2010) 315–322.
[8] A.A. EL-Sherif, Inorg. Chim. Acta 362 (2009) 4991–5000.
[9] R. Malhotra, J. Mehta, J.K. Puri, Cent. Eur. J. Chem. 5 (3) (2007) 858–867.

[10] Z.H. Chohan, Chem. Pharm. Bull. 39 (1991) 1578–1580.
[11] Atta-Ur-Rahman, M.I. Choudhary, W.J. Thomsen, Bioassay Techniques for Drug Development, Harwood Academic, Amsterdam, 2001. 22.
[12] R. Malhotra, J.P. Singh, M. Dudeja, K.S. Dhindsa, J. Inorg. Biochem. 46 (1992) 119–127.
[13] N. Raman, A. Kulandaisamy, C. Thangaraja, Trans. Met. Chem. 28 (2003) 29–36.
[14] S. Singh, R. Malhotra, A. Hooda, K.S. Dhindsa, Bull. Soc. Chim. Belg. 105 (1996) 451–455.
[15] M.T. Dunn, The visible and ultraviolet spectra of complex compounds in modern coordination chemistry (1960).
[16] R. Malhotra, S. Kumar, Jyoti, H.R. Singal, K.S. Dhindsa, Ind. J. Chem. 39A (2004) 421–424.
[17] N. Raman, S. Ravichandran, C. Thangaraja, J. Chem. Sci. 116 (4) (2004) 215–219.
[18] R.L. Dutta, A. Syamal, Elements of Magnetochemistry, third ed., East-West Press, New Delhi, 1992.
[19] N. Raman, A. Julandaisamy, K. Jeya Subramanian, Synth. React. Inorg. Met. Org. Chem. 31 (7) (2001) 1249–1260.
[20] A.W. Coats, J.P. Redfern, Nature 20 (1964) 68–69.